This manuscript was accepted by Appl. Phys. Lett. Click here to see the version of record.

Electrical properties of Si-doped GaN prepared using pulsed sputtering

Yasuaki Arakawa[1], Kohei Ueno[1], Hideyuki Imabeppu[1], Atsushi Kobayashi[1], Jitsuo Ohta[1, 2], and Hiroshi Fujioka[1, 3]

[1]*Institute of Industrial Science, The University of Tokyo, 4-6-1 Komaba, Meguro, Tokyo, 153-8505, Japan*

[2]*PRESTO, Japan Science and Technology Agency (JST), 4-1-8 Honcho, Kawaguchi, Saitama 332-0012, Japan*

[3]*ACCEL, Japan Science and Technology Agency (JST), 5 Sanbancho, Chiyoda-ku, Tokyo 102-0075, Japan*

In this study, we investigated the basic electrical properties of Si-doped wurtzite GaN films prepared using a low-temperature pulsed sputtering deposition (PSD) process. We found that the electron concentration can be controlled in the range between 1.5×10^{16} and 2.0×10^{20} cm^{-3}. For lightly Si-doped GaN ([Si] = 2.1×10^{16} cm^{-3}), the room temperature (RT) electron mobility was as high as 1008 cm^{2}V^{-1}s^{-1}, which was dominantly limited by polar optical phonon scattering. Moreover, we found that heavily Si-doped GaN prepared using PSD exhibited an RT mobility as high as 110 cm^{2}V^{-1}s^{-1} at an electron concentration of 2×10^{20} cm^{-3}, which indicated that the resistivity of this film was almost as small as those of typical transparent conductive oxides such as indium tin oxide. At lower temperatures, the electron mobility increased to 1920 cm^{2}V^{-1}s^{-1} at 136 K, and the temperature dependence was well explained by conventional scattering models. These results indicate that Si-doped GaN

prepared using PSD is promising not only for the fabrication of GaN-based power devices but also for use as epitaxial transparent electrode materials for nitride based optical devices..

This manuscript was accepted by Appl. Phys. Lett. Click here to see the version of record.

GaN has excellent material characteristics for use in power devices, including a high breakdown voltage, high saturation velocity, and high thermal stability. Recent advances in bulk GaN growth technology have facilitated the development of vertical power devices such as Schottky barrier diodes [1,2], p–n junction diodes [3,4], and trench metal–oxide–semiconductor field-effect transistors [5]. One of the key methods used to fabricate these devices is a light n-type doping of GaN with a low residual impurity concentration of the order of 10^{15} cm^{-3} or less. Despite intensive research efforts, the performance of GaN-based power devices has remained insufficient because of an immature epitaxial growth process. The most common method, metal organic chemical vapor deposition (MOCVD), inherently results in GaN that is contaminated by carbon, oxygen, and silicon atoms originating from the metal-organic precursors, susceptor, and reactor walls. The extent of contamination complexly depends on the growth conditions, including the growth temperature, III/V ratio, gas flow rate, and reactor pressure [6]. In particular, several studies on MOCVD have reported an undesirable increase in carbon concentration in GaN with increasing TMGa flow rate [7] or growth rate [8]. By contrast, a new growth technique called pulsed sputtering deposition (PSD) has recently attracted much attention. Recent progress in PSD has enabled the growth of device-quality group-III nitrides at much lower temperatures than those used in a conventional MOCVD process [9-12]. PSD is also a suitable method for growing high-purity GaN because its growth system does not contain carbon or hydrogen atoms in the

This manuscript was accepted by Appl. Phys. Lett. Click here to see the version of record.

source material. In fact, we demonstrated the growth of high-purity p-type GaN with a high room temperature (RT) hole mobility of 34 $cm^2V^{-1}s^{-1}$. This is attributed to a reduction in the amounts of residual impurities such as oxygen, hydrogen, and carbon, which should also be useful for the growth of n-type GaN [13].

In this study, we investigated how the electrical properties of GaN prepared by PSD depend on the Si doping concentrations using temperature-dependent Hall-effect measurements.

Growth of 1-μm-thick Si-doped GaN films was performed by PSD with pulsed magnetron sputtering sources in an N_2/Ar atmosphere. The Si doping concentration in GaN was controlled from 2×10^{16} to 2×10^{20} cm^{-3} by varying Si vapor flux from a solid state single crystalline Si source. Heavily Si-doped samples ([Si] > 1×10^{17} cm^{-3}) were grown on Fe-doped GaN on sapphire prepared by MOCVD with a latter-half threading dislocation density of 10^8 cm^{-2}. Lightly Si-doped samples ([Si] < 1×10^{17} cm^{-3}) were grown on Fe-doped bulk GaN substrates prepared by hydride vapor phase epitaxy with threading dislocation densities on the order of 10^6 cm^{-2}. The concentration of Si dopants in GaN was evaluated by secondary ion mass spectroscopy (SIMS). Details of the growth method have been reported elsewhere [9-14].To fabricate van der Pauw structures, we processed all of the samples into cloverleaf patterns by photolithography and inductively coupled plasma-reactive-ion etching. Ohmic contacts were then formed with Ti/Al/Ti/Au

This manuscript was accepted by Appl. Phys. Lett. Click here to see the version of record.

(20/60/20/50 nm) as electrodes. Temperature-dependent Hall-effect measurements were performed using a ResiTest 8400 (Toyo Corp.) with a liquid-N_2-cooled temperature-variable sample holder. The analytical protocol was based on American Society for Testing and Materials standard F76 [15]; the Hall scattering factor was unity.

Figure 1 shows the RT electron mobilities μ_e of Si-doped PSD GaN as a function of the electron concentration N_e. The RT electron concentration was controlled in the concentration range between 1.5×10^{16} and 2.0×10^{20} cm^{-3} by Si doping. As the Si doping concentration decreased, the RT electron mobility reached 1008 $cm^2V^{-1}s^{-1}$ at an electron concentration of 1.5×10^{16} cm^{-3}. On the other hands, the most heavily doped sample with a Si concentration of 2×10^{20} cm^{-3} exhibited an electron mobility as high as 110 $cm^2V^{-1}s^{-1}$. These results indicate that the resistivity of this film was almost as small as those for typical transparent conductive oxides such as indium tin oxide (ITO). It can be noted that the mobility of 110 $cm^2V^{-1}s^{-1}$ is much higher than that for ITO, which should lead to smaller free-carrier light absorption. These data indicate that the pulse-sputtered Si-doped GaN is a potential transparent electrode material for nitride based optical devices. We also note that the fabrication of such a highly conductive Si-doped GaN material by MOCVD has not been previously reported.

This manuscript was accepted by Appl. Phys. Lett. Click here to see the version of record.

An S-shaped increase in the electron mobility with decreasing electron concentration is clearly observed. This trend can be empirically fit using the Caughey–Thomas equation [16]:

$$\mu(N) = \mu_{\min} + \frac{\mu_{\max} - \mu_{\min}}{1 + \left(\frac{N}{N_g}\right)^{\gamma}}, \quad (1)$$

where $\mu_{\max}$, $\mu_{\min}$, and N_g are the fitting parameters, γ is unity for an n-type semiconductor, and N is the doping concentration with an assumption of $N = N_e$ for simplicity. As evident in Fig. 1, the experimentally obtained data were well fitted by this model with the parameters $\mu_{\max} = 1035$ cm^{2}V^{-1}s^{-1}, $\mu_{\min} = 130$ cm^{2}V^{-1}s^{-1}, and $N_g = 3.0 \times 10^{17}$ cm^{-3}. Mnatsakanov *et al.* also summarized the relationship between electron mobility and electron concentration in MOCVD-grown Si-doped GaN using the same model and extracted fitting parameters as $\mu_{\max}$ = 1000 cm^{2}V^{-1}s^{-1}, $\mu_{\min}$ = 55 cm^{2}V^{-1}s^{-1}, and $N_g = 2.0 \times 10^{17}$ cm^{-3}. The obtained $\mu_{\max}$ for PSD-grown samples was greater than or equal to the values for the state-of-the-art MOCVD-grown samples [17].

Figures 2(a) and (b) show the temperature dependence of electron concentration and mobility, respectively, for Si-doped GaN between 77 and 300 K. For highly Si-doped samples ([Si] > 8×10^{18} cm^{-3}), almost no temperature dependence in the electron concentration exists, as evident in Fig. 2(a). In this doping range, the electron mobility is also independent of the temperature at Si doping concentrations as high as 2×10^{20} cm^{-3}, as

This manuscript was accepted by Appl. Phys. Lett. Click here to see the version of record.

shown in Fig. 2(b). We also observed that almost all Si atoms were active as n-type dopants in GaN, even at a Si concentration as high as 2×10^{20} cm^{-3}. This result indicates that any self-compensation effect [18] and/or the undesirable formation of silicon nitride [19], which are undesirable for heavy Si doping by MOCVD, were negligible in the case of GaN grown using PSD.

For samples doped with lower concentrations of Si ([Si] < 1×10^{17} cm^{-3}), the experimental data related to the temperature dependence of electron concentrations was well fitted under a charge neutrality condition as a non-degenerate n-type semiconductor. The Si doping concentration obtained from the fitting well agreed with the SIMS results. The estimated activation energy of the Si dopant varied from 21 to 24 meV with decreasing Si doping concentration; this behavior is explained by the Coulomb interaction of ionized donors. The details of the fitting results will be summarized elsewhere. With respect to the temperature dependence of the electron mobilities of the samples doped with lower Si contents ([Si] < 1×10^{17} cm^{-3}) shown in Fig. 2(b), the highest peak mobility was 1920 cm^{2}V^{-1}s^{-1} at 136 K for the lightly Si-doped sample ([Si] = 2×10^{16} cm^{-3}). We also observed that the peaks of the electron mobility were shifted toward lower temperatures. This phenomenon is explained by the reduction in the ionized impurity scattering rate with decreasing Si doping concentration. The detailed scattering mechanism is discussed later.

This manuscript was accepted by Appl. Phys. Lett. Click here to see the version of record.

Next, we focus on the electron transport properties of Si-doped GaN with the highest electron mobility in Fig. 2(b). Figures 3(a) and (b) show a reflection high-energy electron diffraction (RHEED) pattern and a 5 × 5 μm^2 atomic force microscopy (AFM) surface image of lightly Si-doped GaN ([Si] = 2 × 10^{16} cm^{-3}) grown on the bulk GaN substrate. A clear streaky RHEED pattern is observed in Fig. 3 (a), which indicates that the growth of Si-doped GaN using PSD proceeded in the two-dimensional growth mode. Figure 3(b) shows an atomically flat step-and-terrace structure with a step width of approximately 1 μm. The root mean square of the surface roughness on the terraces was as low as 0.5 nm. This AFM data corresponds well with the streaky RHEED pattern.

Figure 3(c) shows the detailed temperature dependence of electron mobility between 78 and 400 K and the calculated electron mobility limited by interactions of electrons with impurities, lattice defects, and lattice vibrations. According to Matthiesen's rule, the electron mobility is expressed as $1/\mu_{total} = \sum_i 1/\mu_i$, where μ_{total} and μ_i are the total electron mobility and the electron mobility limited by each scattering process, respectively. For the calculation, expressions for the scattering-limited electron mobilities are taken from the following references: ionized impurity [20], neutral impurity [21], dislocation [22], polar optical phonon [20], acoustic deformation potential [20], and piezoelectric scattering [21]. We assumed that the effects of other scatterings, such as non-polar optical phonon scattering, are negligible on electron mobility. All parameters are defined in Table II. Figure 3(c)

This manuscript was accepted by Appl. Phys. Lett. Click here to see the version of record.

qualitatively clarifies the contribution of each scattering mechanism for temperature dependence of the experimental electron mobility. This calculation result reveals that the RT electron mobility of PSD-grown Si-doped GaN is mainly limited by polar optical phonon scattering. By contrast, at temperatures below 200 K, the ionized impurity scattering became dominant. Reducing the concentration of compensating acceptors is important for further improving the electron mobility in PSD-grown Si-doped GaN. Using high-quality bulk GaN substrates with a low threading dislocation density is also important because the highest low-temperature electron mobility was attained for the sample grown on a substrate with a very low threading dislocation density of 5×10^5 cm^{-2} [25].

In summary, we have grown n-type GaN films with Si dopant concentrations on the order ranging from 10^{16} to 10^{20} cm^{-3} by PSD. The relationship between the RT electron concentration and mobility, as analyzed by the Caughey–Thomas model, revealed μ_{max} and μ_{min} extracted electron mobilities of 1035 and 130 cm^{2}V^{-1}s^{-1}, respectively. For lightly Si-doped GaN ([Si] = 2×10^{16} cm^{-3}), the RT electron mobility was 1008 cm^{2}V^{-1}s^{-1}, which was dominantly limited by polar optical phonon scattering. With a reduction in temperature, electron mobility increases; the peak mobility was 1920 cm^{2}V^{-1}s^{-1} at 136 K, which is mainly limited by ionized impurity scattering. We also observed that heavily Si-doped GaN prepared by PSD exhibited an RT mobility as high as 110 cm^{2}V^{-1}s^{-1} at an electron concentration of 2×10^{20} cm^{-3}, which indicates that the resistivity of this film was almost as small as those of

typical transparent conductive oxides such as ITO. Because the electron mobility of the GaN films is higher than those of the transparent conductive oxides, Si-doped GaN prepared by PSD is a promising epitaxial transparent electrode material for nitride based optical devices.

Acknowledgement

This work was partially supported by the JST ACCEL project and JSPS KAKENHI Grant Number JP16H06414.

References

1. Y. Saitoh, K. Sumiyoshi, M. Okada, T. Horii, T. Miyazaki, H. Shiomi, M. Ueno, K. Katayama, M. Kiyama, and T. Nakamura, Appl. Phys. Express **3**, 081001 (2010).
2. N. Tanaka, K. Hasegawa, K. Yasunishi, N. Murakami, and T. Oka, Appl. Phys. Express **8**, 071001 (2015).
3. Z. Hu, K. Nomoto, B. Song, M. Zhu, M. Qi, M. Pan, X. Gao, V. Protasenko, D. Jena, and H. G. Xing, Appl. Phys. Lett. **107**, 243501 (2015).
4. I. C. Kizilyalli, A. P. Edwards, O. Aktas, T. Prunty, and D. Bour, IEEE Trans. Electron Devices **62**, 414 (2015).
5. T. Oka, T. Ina, Y. Ueno, T. Ina, and K. Hasegawa, Appl. Phys. Express **7**, 021002 (2014).
6. D. D. Koleske, A. E. Wickenden, R. L. Henry, and M. E. Twigg, J. Crystal Growth **242**, 55 (2002).
7. J. T. Chen, U. Forsberg, and E. Janzen, Appl. Phys. Lett. **102**, 193506 (2013).
8. Y. Cao, R. Chu, R. Li, M. Chen, R. Chang, and B. Hughes, Appl. Phys. Lett. **108**, 062103 (2016).
9. K. Ueno, E. Kishikawa, S. Inoue, J. Ohta, H. Fujioka, M. Oshima, and H. Fukuyama, Phys. Stat. Sol. RRL **8**, 256 (2014).

10. E. Nakamura, K. Ueno, J. Ohta, H. Fujioka, and M. Oshima, Appl. Phys. Lett. **104**, 051121 (2014).
11. J. W. Shon, J. Ohta, K. Ueno, A. Kobayashi, and H. Fujioka, Sci. Rep. **4**, 5325 (2014).
12. T. Watanabe, J. Ohta, T. Kondo, M. Ohashi, K. Ueno, A. Kobayashi, and H. Fujioka, Appl. Phys. Lett. **104**, 182111 (2014).
13. Y. Arakawa, K. Ueno, A. Kobayashi, J. Ohta, and H. Fujioka, APL Mater. **4**, 086103 (2016).
14. K. Sato, J. Ohta, S. Inoue, A. Kobayashi, and H. Fujioka, Appl. Phys. Express **2** 011003 (2009).
15. ASTM Standard F76, Test Methods for Measuring Resistivity and Hall Coefficient and Determining Hall Mobility in Single-Crystal Semiconductors (ASTM International, West Conshohocken, PA, 2011).
16. D. M. Caughey and R. E. Thomas, Proc. IEEE **55**, 2192 (1967).
17. T. T. Mnatsakanov, M. E. Levinshtein, L. I. Pomortseva, S. N. Yurkov, G. S. Simin, and M. A. Khan, Solid-State Electron. **47**, 111 (2003).
18. I. Halidou, Z. Benzarti, Z. Chine, T. Boufaden, and B. E. Jani, Microelectron. J. **32**, 137 (2001).
19. A. Dadgar, J. Bläsing, A. Diez, and A. Krost, Appl. Phys. Express **4**, 011001

(2011).

20. K. Seeger, *Semiconductor Physics: An introduction* (Springer, Vienna, 2004).

21. E. C. H. Kyle, S. W. Kaun, P. G. Burke, F. Wu, Y. R. Wu, and J. S. Speck, J. Appl. Phys. **115**, 193702 (2014).

22. H. M. Ng, D. Doppalapudi, T. D. Moustakas, N. G. Weimann, and L. F. Eastman, Appl. Phys. Lett. **73**, 821 (1998).

23. D. C. Look and J. R. Sizelove, Appl. Phys. Lett. **79**, 1133 (2001).

24. D. Huang, F. Yun, M. A. Reshchikov, D. Wang, H. Morkoç, D. L. Rode, L. A. Farina, Ç. Kurdak, K. T. Tsen, S. S. Park, and K. Y. Lee, Solid-State Electron. **45**, 711 (2001).

25. D. C. Look, C. E. Stutz, R. J. Molnar, K. Saarinen, and Z. Liliental-Weber, Solid State Commun. **117**, 571 (2001).

Figures

Figure 1. The relationship between electron concentration and electron mobility of PSD-grown Si-doped GaN. The open blue circles and the red solid line represent the experimental data and the fitting result obtained using the Caughey–Thomas model [16], respectively.

Figure 2. Temperature dependence of (a) electron concentration and (b) electron mobility in PSD-grown Si-doped GaN. In Fig. 2(a), for lower Si-doped samples ([Si] < 1×10^{17} cm^{-3}), the fitting results based on a charge neutrality condition were also shown in solid lines.

Figure 3. (a) RHEED pattern and (b) 5×5 μm^2 AFM surface image of lightly Si-doped GaN ([Si] = 2×10^{16} cm^{-3}) grown on the bulk GaN substrate. (c) The temperature dependence of the experimental electron mobility in lightly Si-doped GaN ([Si] = 2×10^{16} cm^{-3}), the calculated electron mobilities limited by individual scattering mechanism, and the total electron mobility obtained on the basis of Matthiesen's rule.

1 Table I. Material parameters for the calculation of the electron mobilities limited by the

2 individual scattering mechanism.

Parameter	Literature value
Effective mass	0.22 [24]
Static dielectric constant	9.5 [25]
High frequency dielectric constant	5.15 [23]
Longitudinal elastic constant (GPa)	371 [21]
Transversal elastic constant (GPa)	126 [21]
Acoustic deformation potential (eV)	9.2 [23]
Polar phonon Debye temperature (K)	1057 [23]
Distance between acceptor-like trap centers along a dislocation (Å)	5.185 [21]

3

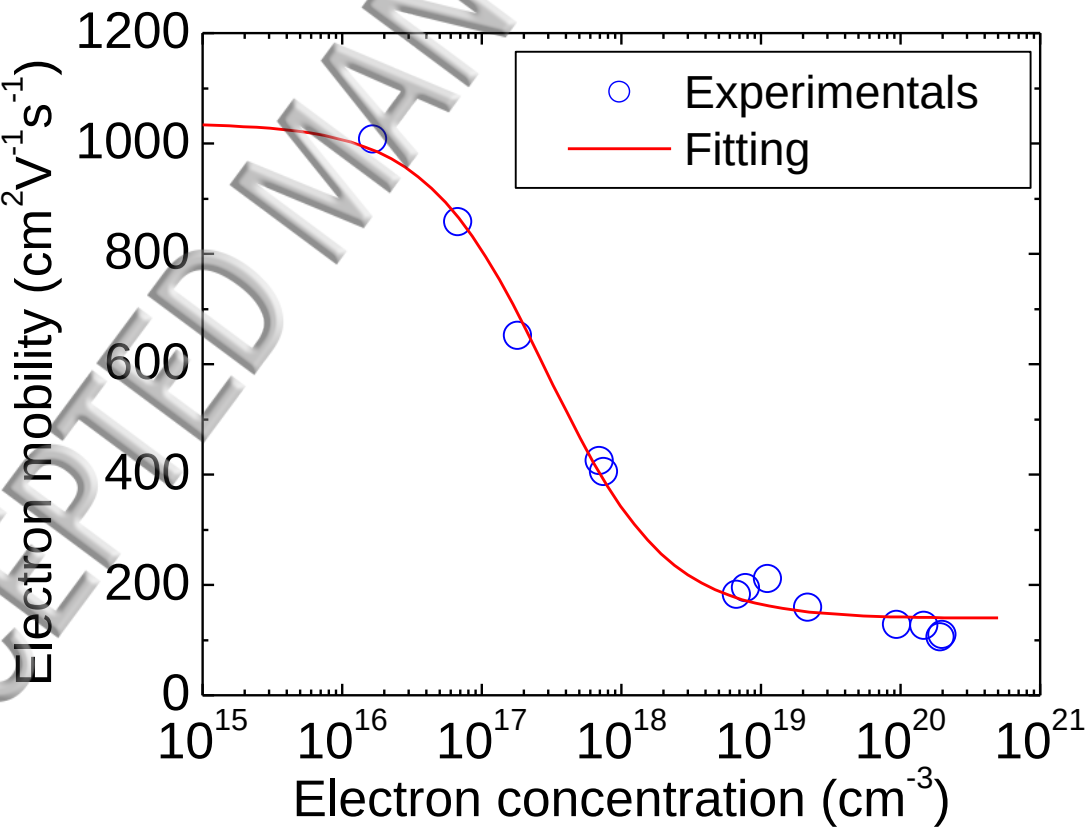

Y. Arakawa *et al*., Figure 1

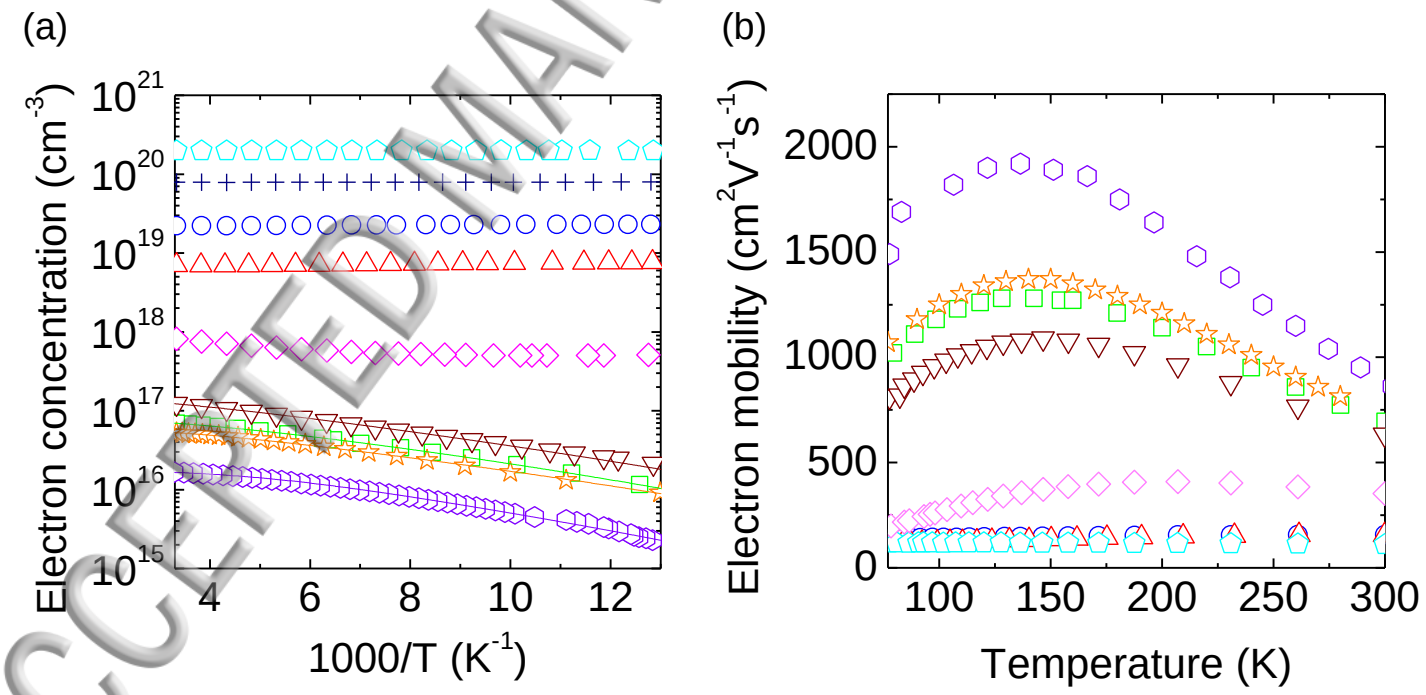

Y. Arakawa *et al.*, Figure 2

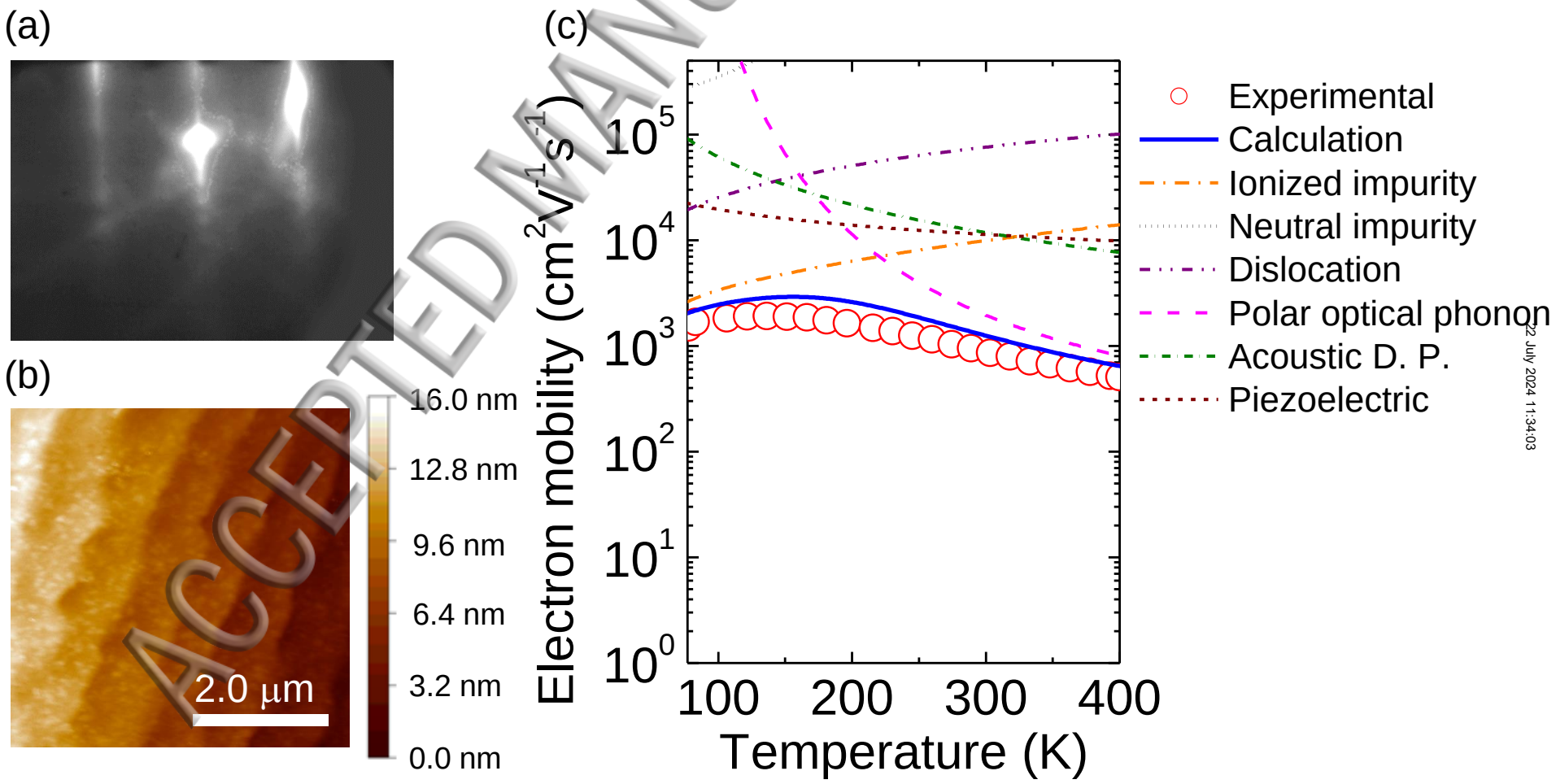

Y. Arakawa *et al*., Figure 3